

FTIR Spectroscopic Study of the Cl-Atom-Initiated Reactions of Ethylene Oxide in O₂/N₂ Diluent

J. Chen, V. Young, P. A. Hooshiyar, and H. Niki*

Centre for Atmospheric Chemistry and Department of Chemistry, York University, 4700 Keele Street, North York, Ontario, Canada M3J 1P3

M. D. Hurley

SRL-E3083, Ford Motor Company, Dearborn, Michigan 48121-2053

Received: August 18, 1994; In Final Form: December 16, 1994[®]

A long-path FTIR spectroscopic study of the Cl-atom-initiated reactions of ethylene oxide ($\text{H}_2\text{C}-\text{O}-\text{CH}_2$) was carried out at 297 ± 2 K in the photolysis (300 nm) of mixtures containing $\text{H}_2\text{C}-\text{O}-\text{CH}_2$ and Cl_2 in both the torr and millitorr ranges in 700 Torr of N₂ or O₂/N₂ diluent. In 700 Torr of N₂, the only primary product detected was $\text{H}_2\text{C}-\text{O}-\text{CHCl}$, formed via (1) $\text{Cl} + \text{H}_2\text{C}-\text{O}-\text{CH}_2 \rightarrow \text{H}_2\text{C}-\text{O}-\text{CH} + \text{HCl}$ followed by (2) $\text{H}_2\text{C}-\text{O}-\text{CH} + \text{Cl}_2 \rightarrow \text{H}_2\text{C}-\text{O}-\text{CHCl} + \text{Cl}$. Thus, the cyclic oxiranyl radical $\text{H}_2\text{C}-\text{O}-\text{CH}$ formed in reaction 1 was sufficiently long-lived to react with Cl_2 . An upper limit value of $k_3 \leq 2 \times 10^4 \text{ s}^{-1}$ has been estimated for the rate constant of the possible oxiranyl-to-vinoy isomerization: (3) $\text{H}_2\text{C}-\text{O}-\text{CH} \rightarrow \text{CH}_2\text{CHO}$. The $\text{H}_2\text{C}-\text{O}-\text{CHCl}$ yield decreased with increase in added O₂ due to the occurrence of reaction 4: (4) $\text{H}_2\text{C}-\text{O}-\text{CH} + \text{O}_2 (+ \text{M}) \rightarrow \text{H}_2\text{C}-\text{O}-\text{C}(\text{OO})\text{H} (+ \text{M})$. A value of $k_2/k_4 = 2.0 \pm 0.4$ was derived from the O₂ dependence of the $\text{H}_2\text{C}-\text{O}-\text{CHCl}$ yield. In 700 Torr of air, the observed products included C–O–C bonded compounds $\text{HC}(\text{O})\text{OCHO}$ and $\text{CH}_2(\text{OH})\text{OCHO}$, and one-carbon species CO, CO₂, HCHO, and $\text{HC}(\text{O})\text{OH}$, but not C–C bonded products. The preferential formation of C–O–C rather than C–C bonded products suggests the predominant cleavage of the C–C bond rather than the C–O bond in a three membered ring precursor radical. The most likely candidate is the cyclic radical $\text{H}_2\text{C}-\text{O}-\text{C}(\text{O})\text{H}$ formed via self-reaction, i.e., $2\text{H}_2\text{C}-\text{O}-\text{C}(\text{OO})\text{H} \rightarrow 2\text{H}_2\text{C}-\text{O}-\text{C}(\text{O})\text{H} + \text{O}_2$. A detailed mechanism is proposed for the oxidation of the $\text{H}_2\text{C}-\text{O}-\text{C}(\text{O})\text{H}$ radical leading to the formation of the observed products.

Introduction

The Cl-atom-initiated reactions of ethylene oxide ($\text{H}_2\text{C}-\text{O}-\text{CH}_2$) were studied previously by Bartels et al., using the discharge flow–mass spectrometric method at 298 K in 1 Torr of diluent He.¹ Interestingly, they reported evidence for the occurrence of both the abstraction and addition channels for the $\text{Cl} + \text{H}_2\text{C}-\text{O}-\text{CH}_2$ reaction with an overall rate constant of $2.8 \times 10^{-11} \text{ cm}^3 \text{ molecule}^{-1} \text{ s}^{-1}$ and also for the formation of three isomeric C₂H₃O radicals (i.e., cyclic oxiranyl $\text{H}_2\text{C}-\text{O}-\text{CH}$, vinoy CH_2CHO , and acetyl CH_3CO) within 5×10^{-3} s of reaction time following the H-atom abstraction. The reaction pathways and the corresponding products identified mass spectrometrically by Bartels et al. are shown schematically in Figure 1. Since the products were not quantified in their study, the relative importance of various competing channels remains to be determined. In view of the importance of these elementary reactions in atmospheric chemistry, we have undertaken an FTIR-based product study of the Cl-atom-initiated reactions of ethylene oxide at 297 K in the presence of 700

Torr of N₂ and O₂/N₂ mixtures. The results thus obtained are presented below.

Experimental Section

The experimental facility and procedures have previously been described in detail.² In brief, a Pyrex glass cylinder (5 cm diameter, 50 cm long, and 100 cm path length) surrounded by UV lamps (GE F30T8/BLB; 300 nm) was used as the IR cell/photochemical reactor for experiments with reactant partial pressures in the torr range; another Pyrex glass cylinder (30 cm diameter, 2 m long, and 180 m path length) surrounded by UV lamps (GE F40T12/BLB; 300 nm) was used for experiments with reactant pressure in the millitorr range. Infrared spectra in the 500–3700 cm^{−1} frequency range were typically recorded after every 5 or 15 s of irradiation at 1/16 cm^{−1} resolution with a Ge-coated KBr beam splitter and a liquid He cooled Cu–Ge detector.

Ethylene oxide (99%, Matheson) was used after trap-to-trap distillation over liquid N₂. Cl₂ (99.5%, Matheson), N₂ (99.99%, Matheson), O₂ (99.99%, Matheson), and zero air (ultra zero grade, Air Monitoring) were used as received. Cl atoms were generated by the UV (300 ≤ λ ≤ 400 nm) photolysis of Cl₂. All the reference IR spectra for the products reported in this

* To whom correspondence should be addressed.

[®] Abstract published in *Advance ACS Abstracts*, February 15, 1995.

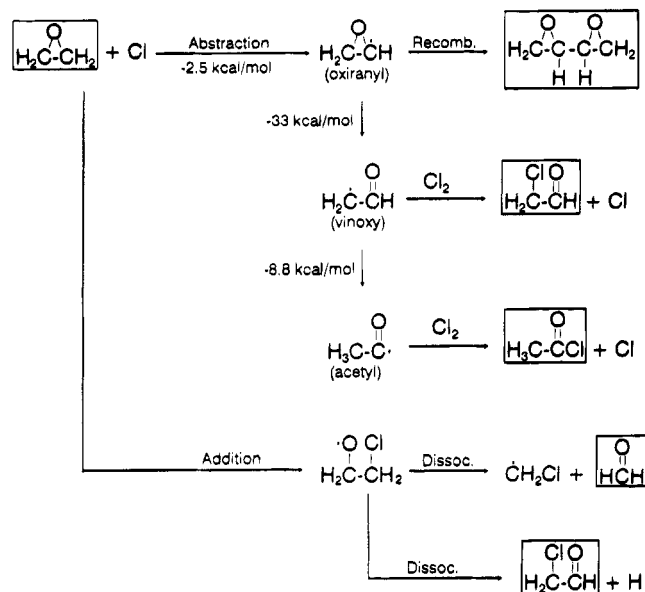
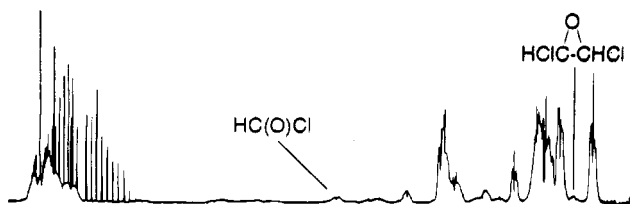


Figure 1. Mechanism for the Cl-atom-initiated reactions of ethylene oxide in 1 Torr of He proposed by Bartels et al. (ref 1).

(A) C₂H₄O (1 torr)/Cl₂ (0.5 torr)/N₂ (700 torr)



(B) After 15 sec Irradiation



(C) [(B) - (A)]

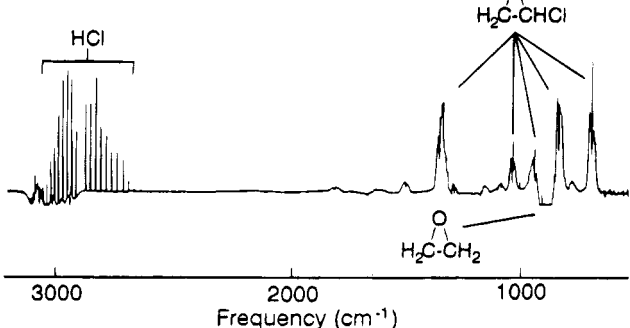


Figure 2. Spectral data in the frequency region 500–3200 cm⁻¹ obtained from the photolysis of a mixture containing 1.0 Torr of ethylene oxide and 0.5 Torr of Cl₂ in 700 Torr of N₂: (A) before irradiation, (B) after 15 s irradiation, (C) difference spectrum (B–A).

paper were available from previous studies, except for four compounds: monochloroethylene oxide (H₂C–O–CHCl), dichloroethylene oxide (HCIC–O–CHCl), chloromethyl formate (CH₂ClOCHO), and hydroxymethyl formate (CH₂(OH)OCHO). These products were identified on the basis of literature information, and their concentrations were estimated from material balance, as described below.

Results and Discussion

Three sets of experiments were performed: (i) photolysis of mixtures of H₂C–O–CH₂ (0.5–1.5 Torr) and Cl₂ (0.5–2.0 Torr) in 700 Torr of pure N₂; (ii) photolysis of mixtures of H₂C–O–CH₂ (0.5–1.5 Torr) and Cl₂ (0.5 Torr), as well as H₂C–O–CH₂ (5–30 mTorr) and Cl₂ (20 mTorr), in 700 Torr of air; and (iii) photolysis of mixtures of H₂C–O–CH₂ (1 Torr), Cl₂ (0.5 Torr), and O₂ (2–140 Torr) diluted in N₂ to a total pressure of 700 Torr. To ensure thorough mixing of the reactants, the reactant mixtures were kept in the reactor in the dark for about 10 min prior to irradiation. Neither changes in the reactant concentrations nor the formation of new products was observed during this dark aging period.

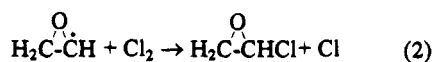
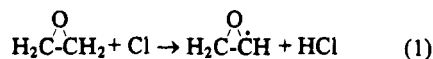
(i) Reactions in N₂. Typical infrared spectral data obtained in the photolysis of ethylene oxide and Cl₂ in N₂ diluent are shown in Figure 2. Parts A and B correspond to the spectra recorded before and after 15 s irradiation of a mixture initially

containing H₂C–O–CH₂ (1 Torr) and Cl₂ (0.5 Torr); Figure 2C is the difference spectrum (2B–2A). After 15 s irradiation, 434 mTorr of H₂C–O–CH₂ was consumed, and among the products observed were HC(O)Cl (9 mTorr), HCl (446 mTorr), and two other compounds whose desynthesized spectra are shown in Figure 3A,B. The spectrum in Figure 3A can be

readily assigned to monochloroethylene oxide, H₂C–O–CHCl, by comparison with the liquid-phase spectrum reported by Rannug et al.³ They observed three strong sharp peaks at 910, 1010, and 1330 cm⁻¹, consistent with those in Figure 3A. The two conspicuous peaks that we observe at 805 and 654 cm⁻¹ were presumably obscured by the solvent CCl₄ used in their work. The spectrum shown in Figure 3B exhibits bands at 921

and 1321 cm⁻¹ (C–O–C ring deformation) and at 747 and 801 cm⁻¹ (C–Cl stretch). On the basis of the similarity to the liquid-phase spectra observed by Derkosch et al.,⁴ this spectrum has been assigned to dichloroethylene oxide, HCIC–O–CHCl. The yields of mono- and dichloroethylene oxides were derived from the carbon balance before and after irradiation. In runs such as those shown in Figure 2, the yields of mono- and dichloroethylene oxide were 93 ± 5% and 4 ± 1% (average of three runs), respectively (cf. Table 1). Product yields derived from three runs with similar reactant concentrations and conversions are listed in Table 1. About 97% of the carbon-containing products are chlorinated ethylene oxides, the remainder being HC(O)Cl.

The observation of monochloroethylene oxide as the dominant product can be attributed to H-atom abstraction by Cl atom to yield HCl and the oxiranyl H₂C–O–CH radical, followed by the Cl₂ reaction, i.e., reactions 1 and 2.



Similarly, dichloroethylene oxide was formed in the present system from monochloroethylene oxide via the analogous chlorination mechanism. In Figure 4, [HCl] is plotted against {[H₂C–O–CHCl] + 2[HCIC–O–CHCl] + [HC(O)Cl]}. The slope of the line is 0.99 ± 0.05, which demonstrates that the

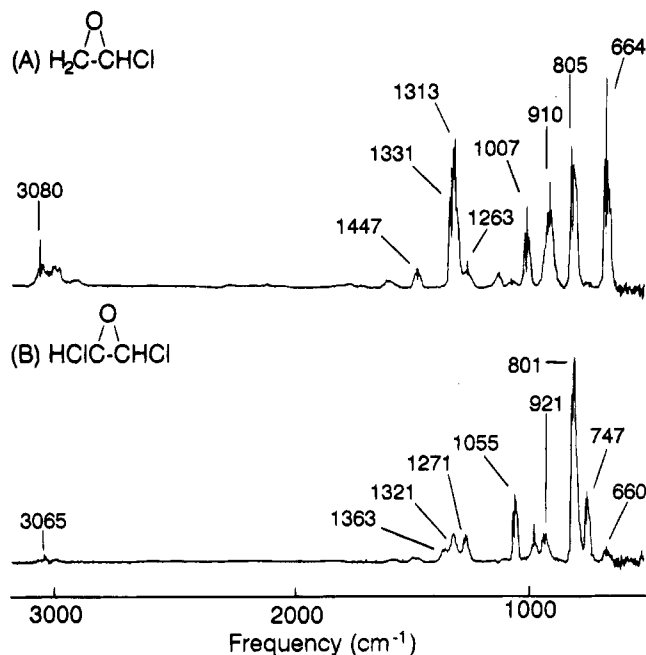


Figure 3. IR spectra of (A) chloroethylene oxide and (B) dichloroethylene oxide obtained as residual spectra from the irradiation of mixtures containing $\text{H}_2\text{C}-\text{O}-\text{CH}_2$ and Cl_2 in 700 Torr of N_2 .

TABLE 1: Summary of Product Yields

	diluent			
	N_2 (700 Torr)	air (700 Torr)	air (700 Torr)	O_2 (10 Torr)/ N_2 (690 Torr)
[reactant] (Torr)	ca. 1	ca. 1	ca. 0.01	ca. 1
irradiation (s)	15	120	50	60
$\Delta[\text{H}_2\text{C}-\text{O}-\text{CH}_2]$ (%)	43.4	17.5	5.4	19.7
product	yield (%)			
CO		33 ± 3	36 ± 4	53 ± 5
CO_2		5 ± 1	6 ± 1	7 ± 1
HCHO		4 ± 1	7 ± 1	3 ± 1
$\text{HC}(\text{O})\text{Cl}$	3 ± 1	<0.5	<0.5	4 ± 1
$\text{HC}(\text{O})\text{OH}$		18 ± 2	14 ± 2	40 ± 4
$\text{H}_2\text{C}-\text{O}-\text{CHCl}$	93 ± 5			8 ± 1
$\text{HCIC}-\text{O}-\text{CHCl}$	4 ± 1			
CH_2ClCHO				6 ± 2
$\text{HC}(\text{O})\text{OCHO}$		61 ± 4	61 ± 4	19 ± 2
$\text{CH}_2(\text{OH})\text{OCHO}$		9 ± 3	9 ± 3	13 ± 4

^a The yields listed for each diluent are average of three runs with similar reactant concentrations and conversions.

HCl yield is in excellent agreement with the stoichiometric relation for the products arising from H-abstraction (reaction 1). $\text{HC}(\text{O})\text{Cl}$ is a minor product whose source is not apparent from the present data. Presumably, it was not produced by the heterogeneous decay of chloroethylene oxide and dichloroethylene oxide on the reactor walls, since its concentration did not change during a 10 min dark aging following irradiation.

Interestingly, yields of HCHO and CH_2ClCHO were below the estimated detection limit of 1 and 2 mTorr, respectively, corresponding to 0.3% and 0.5% of the $\text{H}_2\text{C}-\text{O}-\text{CH}_2$ reacted (see Table 1). HCHO and CH_2ClCHO are products of the primary reaction channel postulated by Bartels et al.,¹ i.e., Cl-atom addition followed by unimolecular dissociation (Figure

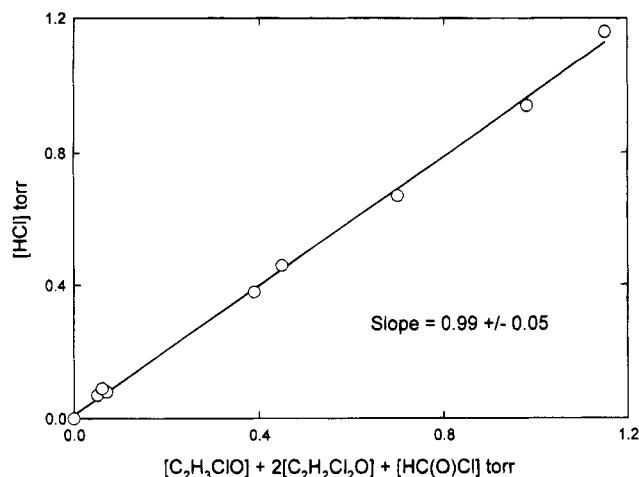
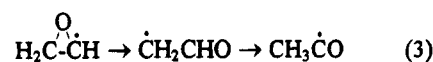


Figure 4. Plot of $[\text{HCl}]$ vs $\{[\text{H}_2\text{C}-\text{O}-\text{CHCl}] + 2[\text{HCIC}-\text{O}-\text{CHCl}] + [\text{HC}(\text{O})\text{Cl}]\}$ for irradiation of mixtures containing $\text{H}_2\text{C}-\text{O}-\text{CH}_2$ and Cl_2 in N_2 .

1). Bartels et al. also reported evidence for isomerization of the oxiranyl radical $\text{H}_2\text{C}-\text{O}-\text{CH}$ to the vinoxy radical CH_2-CHO and to the acetyl radical CH_3CO (reaction 3).



They identified the chlorinated products CH_2ClCHO and CH_3CClO , which arise from the Cl_2 reactions of CH_2CHO and CH_3CO radicals. In the present experiment, these compounds were, if formed, below the detection limit of 2 mTorr, i.e., 0.5% yield. The difference in observed product distribution may be attributed to the higher Cl_2 concentrations used in the present study (0.5–2 Torr as opposed to 10^{-5} – 10^{-4} Torr used by Bartels et al.). Thus,

in our experiments, the oxiranyl $\text{H}_2\text{C}-\text{O}-\text{CH}$ radical reacted with Cl_2 rather than undergoing isomerization, the estimated rate constant ratio k_2/k_3 being $\leq 165 \text{ Torr}^{-1}$. If the rate constant for reaction 2 is at the collision limit, i.e., $1 \times 10^{-10} \text{ cm}^3 \text{ molecule}^{-1} \text{ s}^{-1}$, then the rate constant for isomerization is $k_3 \leq 2 \times 10^4 \text{ s}^{-1}$, giving a lower limit for the lifetime of oxiranyl radicals vs isomerization of $5 \times 10^{-5} \text{ s}$.

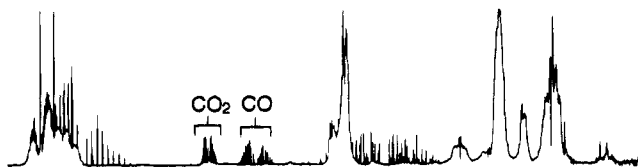
(ii) **Reactions in Air.** Illustrated in Figure 5 are the spectral data obtained in the photolysis of a mixture containing

$\text{H}_2\text{C}-\text{O}-\text{CH}_2$ (1 Torr) and Cl_2 (0.5 Torr) in 700 Torr of synthetic air. Figure 5A,B shows the spectra recorded before and after 2 min irradiation, respectively, and Figure 5C is the difference spectrum (5B–5A). After 2 min irradiation, 175 mTorr of ethylene oxide was consumed, and among the products were formic anhydride ($\text{HC}(\text{O})\text{OCHO}$, 108 mTorr), $\text{HC}(\text{O})\text{OH}$ (31 mTorr), HCHO (5 mTorr), CO (57 mTorr), CO_2 (10 mTorr), $\text{HC}(\text{O})\text{Cl}$ (2 mTorr), HCl (130 mTorr), and H_2O_2 (73 mTorr). In terms of carbon balance, these products account for greater

than 90% of the $\text{H}_2\text{C}-\text{O}-\text{CH}_2$ reacted. A residual spectrum, shown in Figure 6A, was obtained by subtracting the spectra of these products from Figure 5C. This residual spectrum reveals peaks at 1053, 1116, 1170, 1750, 2940, and 3470 cm^{-1} and matches well the spectra reported by Niki et al.⁵ and Su et al.⁶ for hydroxymethyl formate ($\text{CH}_2(\text{OH})\text{OCHO}$). The concentration of $\text{CH}_2(\text{OH})\text{OCHO}$ was derived from the material balance. A summary of average product yields in air, derived from three runs with the similar reactant concentrations and conversions, is listed in Table 1 for reactant concentrations in both the torr and the millitorr ranges.

(A) C₂H₄O (1 torr)/Cl₂ (0.5 torr)/Air (700 torr)

(B) After 2 min Irradiation



(C) [(B) - (A)]

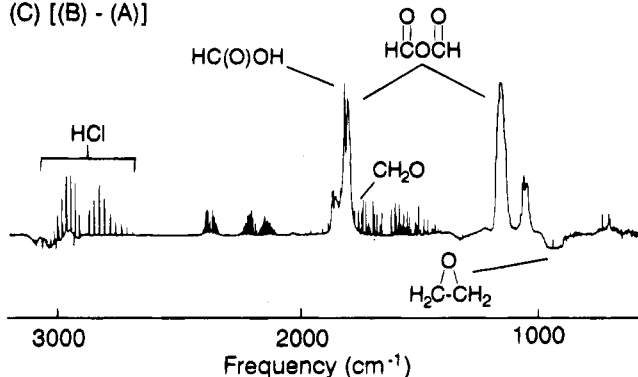


Figure 5. Spectral data in the frequency region 500–3200 cm⁻¹ obtained from the photolysis of a mixture containing 1 Torr of ethylene oxide and 0.5 Torr of Cl₂ in 700 Torr of air: (A) before irradiation, (B) after 2 min irradiation, (C) difference spectrum (B–A).

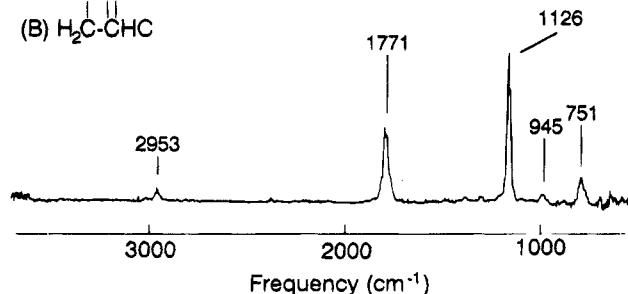
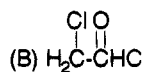
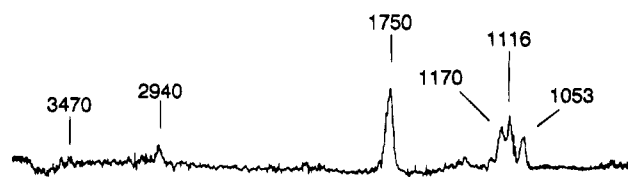
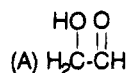
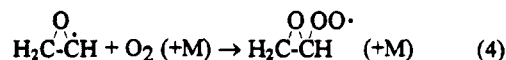


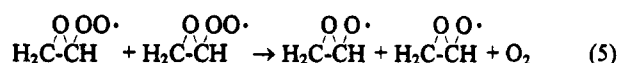
Figure 6. IR spectra of (A) hydroxymethyl formate and (B) chloromethyl formate obtained as residual spectra from the irradiation of H₂C–O–CH₂ and Cl₂ in 700 Torr of O₂/N₂ diluent.

It can be noted in Table 1 that approximately 70% of the H₂C–O–CH₂ consumed led to the formation of acyclic compounds with a C–O–C bond, while the remainder gave rise to compounds containing only one carbon. This degradation of

the three-membered ring of H₂C–O–CH₂ in air is in contrast to the results obtained in N₂, where the ring remained largely intact. In addition, only a minute yield of the chlorinated product HC(O)Cl and no products containing a C–C bond were observed in these runs. Thus, in 700 Torr of air, the oxiranyl radical reacted predominantly with O₂.

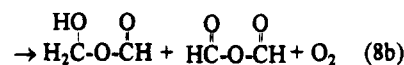
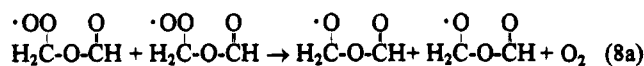
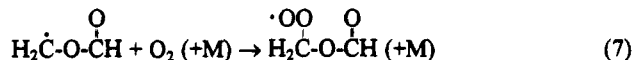
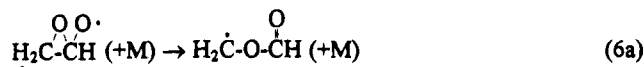


The resulting oxiranylperoxy H₂C–O–C(OO)H radical is expected to behave similarly to the alkyl peroxy radicals^{7,8} and undergo self-reaction to form mainly the oxiranyloxy H₂C–O–C(O)H radical.



In addition to reaction 5, there are other possible self-reaction channels forming molecular products, which should be identifiable by their characteristic C–O–C ring deformations (800–900 cm⁻¹, 1300 cm⁻¹),^{4,9} O–H stretches (near 3600 cm⁻¹)⁸ and C=O stretches (1900 cm⁻¹).¹⁰ Such compounds were not detected in the present study. Thus, reaction 5 appears to be the dominant channel for the self-reaction of the oxiranylperoxy H₂C–O–C(OO)H radical.

The observation of ring-opening products such as formic anhydride, HC(O)OCHO, as the major product indicates cleavage of the C–C bond rather than the C–O bond of the oxiranyloxy H₂C–O–C(O)H radical, reaction 6a followed by reactions 7–9. We propose reactions 8b and 9 as the elementary reactions responsible for the formation of formic anhydride and reaction 8b for hydroxymethyl formate.



Note that glyoxal HC(O)CHO could be formed by reaction 6b followed by H₂C(O*)CHO + O₂ → HC(O)CHO + HOO·. However, HC(O)CHO was not detected among the products, and its yield was less than 1% of the ethylene oxide consumed. Thus, reaction 6b is relatively unimportant, and reaction 6a is the predominant channel for decay of the H₂C–O–C(O)H radical. The relative value of ΔH for the competing channels 6a and 6b was estimated by comparing the ΔH_f values of the H₂C–O–CHO and H₂C(O*)CHO radicals. The ΔH_f values of

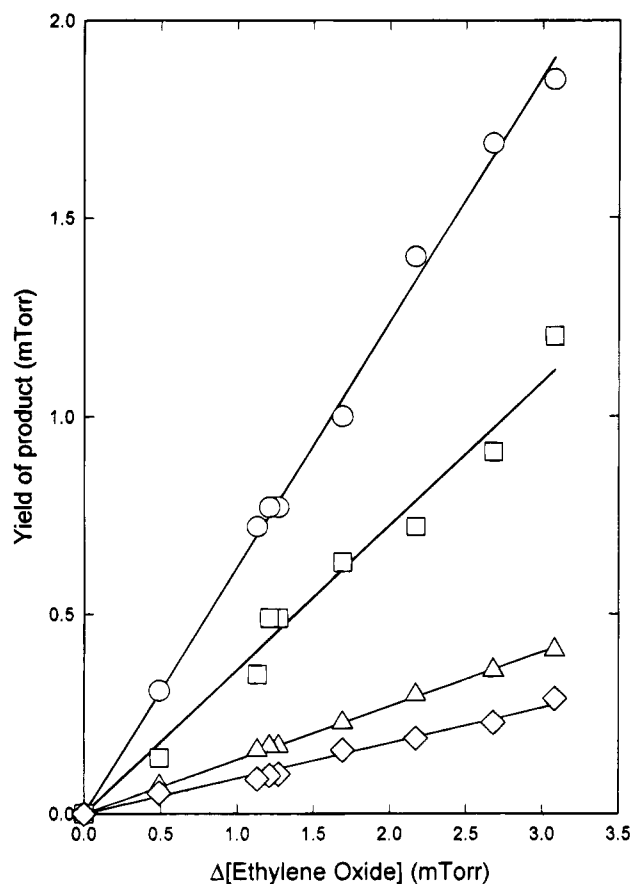


Figure 7. Plot of the product yields as functions of the $\text{H}_2\text{C}-\text{O}-\text{CH}_2$ consumed in the photolysis of $\text{H}_2\text{C}-\text{O}-\text{CH}_2$ and Cl_2 in 700 Torr of air: (○) HC(O)OCHO , (□) CO , (Δ) HC(O)OH , (◇) $\text{H}_2\text{C(OH)OCHO}$.

the $\text{H}_2\text{C}-\text{O}-\text{CHO}$ and $\text{H}_2\text{C(O}^*)\text{CHO}$ radicals were estimated by subtracting the bond dissociation energies $\Delta H(\text{H}-\text{C})$ and $\Delta H(\text{H}-\text{O})$ from the ΔH_f values of molecules $\text{H}_3\text{C}-\text{O}-\text{CHO}$ and $\text{H}_2\text{C(OH)CHO}$, respectively. By using the AM1 method,¹¹ ΔH_f values for $\text{H}_3\text{C}-\text{O}-\text{CHO}$ and $\text{H}_2\text{C(OH)CHO}$ were estimated to be -91.1 and -86.7 kcal/mol, respectively. We chose the bond dissociation energies $\Delta H(\text{H}-\text{C}) = 93.0$ kcal/mol¹² from $\text{CH}_3-\text{O}-\text{CH}_3$ and $\Delta H(\text{H}-\text{O}) = 104.2$ kcal/mol¹³ from $\text{C}_2\text{H}_5\text{OH}$. Values of ΔH_f thus derived are 1.9 kcal/mol for $\text{H}_2\text{C}-\text{O}-\text{CHO}$ and 17.5 kcal/mol for $\text{H}_2\text{C(O}^*)\text{CHO}$. Thus, the $\text{H}_2\text{C}-\text{O}-\text{CHO}$ radical is about 16 kcal/mol more stable than the $\text{H}_2\text{C(O}^*)\text{CHO}$ radical, and channel 6a is thermodynamically favored over channel 6b.

Plotted in Figure 7 are the observed yields of the main products HC(O)OCHO , CO , $\text{H}_2\text{C(OH)OCHO}$, and HC(O)OH , as a function of $\text{H}_2\text{C}-\text{O}-\text{CH}_2$ conversion. Product yields increase linearly with the conversion of $\text{H}_2\text{C}-\text{O}-\text{CH}_2$, indicating the absence of secondary reactions involving these products. The product yields listed in Table 1 were derived by a linear least-squares analysis of these experimental data.

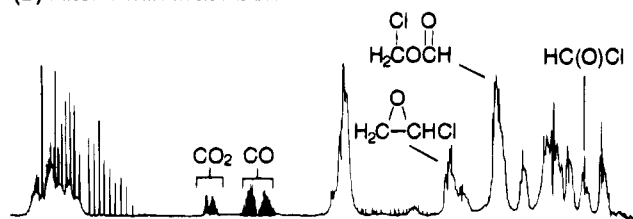
According to Table 1, the yields of HC(O)OCHO and $\text{CH}_2(\text{OH})\text{OCHO}$ in air are 61% and 9%, respectively, of the $\text{H}_2\text{C}-\text{O}-\text{CH}_2$ reacted. Reaction 8b alone would produce equimolar yields of these products. The formation of HC(O)OCHO in a large excess over $\text{CH}_2(\text{OH})\text{OCHO}$ can thus be taken as a measure of the extent to which reaction 9 occurs.

It should be mentioned that both HC(O)OCHO and $\text{CH}_2(\text{OH})\text{OCHO}$ are well-known products of the $\text{O}_3 + \text{C}_2\text{H}_4$ reaction

(A) $\text{C}_2\text{H}_4\text{O}$ (1 torr)/ Cl_2 (0.5 torr)/ O_2 (10 torr)/ N_2 (690 torr)



(B) After 1 min Irradiation



(C) [(B) - (A)]

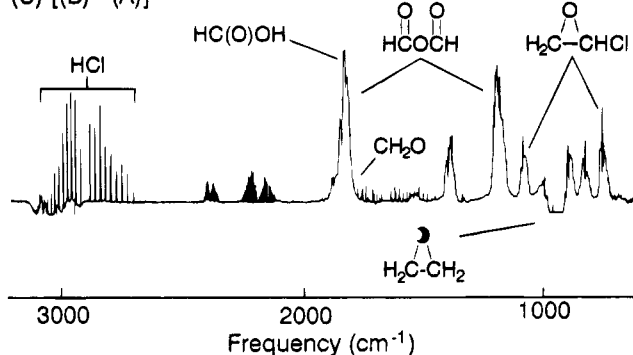


Figure 8. Spectral data obtained in the frequency region 500–3200 cm^{-1} obtained from the photolysis of a mixture containing 1 Torr of $\text{H}_2\text{C}-\text{O}-\text{CH}_2$ and 0.5 Torr of Cl_2 in 10 Torr of O_2 and 700 Torr of N_2 : (A) before irradiation, (B) after 1 min irradiation, (C) difference spectrum (B–A).

in the presence of air.^{5,6,14,15} Although the exact mechanism is still uncertain, the formation of $\text{CH}_2(\text{OH})\text{OCHO}$ has been attributed to the reaction of the Criegee intermediate $\text{H}_2\text{C(O)O}$ with HCHO , both of which are the primary products in the ozonolysis of C_2H_4 .^{5,6} In the $\text{O}_3 + \text{C}_2\text{H}_4$ reaction, the formation of HC(O)OCHO coincided with the slow heterogeneous decay of $\text{CH}_2(\text{OH})\text{OCHO}$ on the reactor walls, and therefore, it was not a gas-phase product.⁵ Such mechanisms are not compatible with our observations in the present reaction system.

As shown in Table 1, a number of single carbon products (CO , CO_2 , HCHO , and HC(O)OH) are produced in substantial yields. Although the present study does not permit quantitative account of the elementary reactions leading to their production, these products were formed either directly, via secondary reactions involving unimolecular dissociation of some of the precursor peroxy or oxy radicals mentioned above, or via secondary Cl-atom reactions of products. For example, the $\text{H}_2\text{C(O}^*)-\text{O}-\text{CHO}$ radical may undergo unimolecular dissociation to produce $\text{H}_2\text{CO}_2 + \text{CHO}$ or $\text{H} + \text{CO}_2 + \text{CH}_2\text{O}$. The CHO radical can react with O_2 to yield HOO and CO and with Cl_2 to yield HC(O)Cl . The observation of H_2O_2 among the major products indicates the self-reaction HOO radicals forming H_2O_2 . For example, 73 mTorr of H_2O_2 was formed when 175 mTorr of ethylene oxide was consumed in air (cf. Figure 5). Under such conditions, it is likely that some of the HC(O)OH was produced via the HOO reaction with HCHO .^{16,17} In fact, HC(O)OH and HCHO are the only compounds that do not give nearly identical yields in the torr and millitorr ranges of reactant pressures (cf. Table 1). While the yields of each of

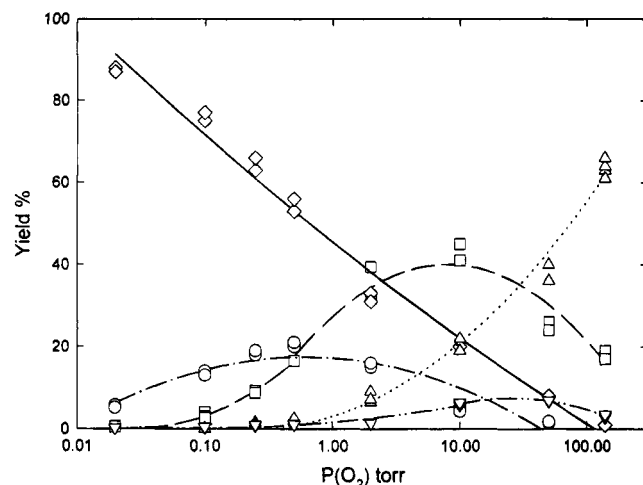


Figure 9. Percentage yields of main products plotted as the function of O_2 pressure: (Δ) $HC(O)OCHO$, (\diamond) $H_2C-O-CHCl$, (\square) $HC(O)OH$, (\circ) $CH_2ClOCHO$, (∇) $HCHO$.

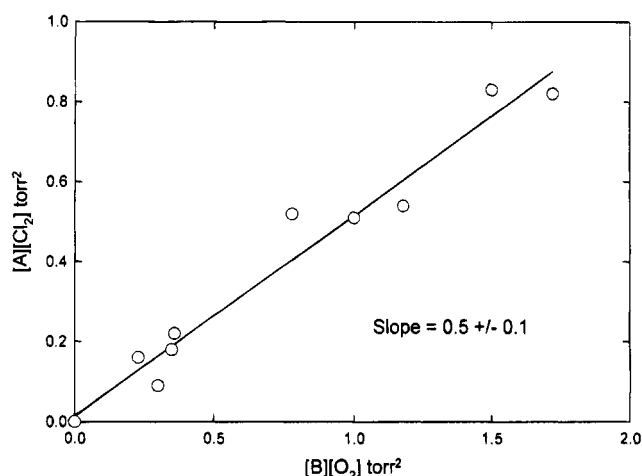
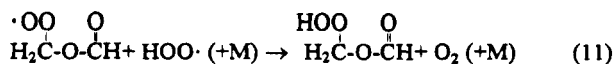
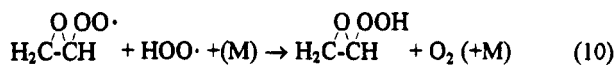


Figure 10. $[A][Cl_2]$ plotted against $[B][O_2]$. Data from six experimental runs. The slope represents k_2/k_4 , where: $[A] = [HC(O)OCHO] + [CH_2(OH)OCHO] + [CH_2ClOCHO] + [HC(O)OH]/2 + [CH_2O]/2 + [CO]/2 + [CO_2]/2$ and $[B] = [H_2C-O-CHCl] + [HC(O)O-CHCl]$.

these compounds varied, their sum was nearly constant. This is consistent with more favorable conversion of $HCHO$ to $HC(O)OH$ by $HOO\cdot$ at higher $HCHO$ concentrations. Also, $HOO\cdot$ may react with other peroxy radicals present, e.g., reactions 10 and 11.



However, no IR peaks characteristic of the peroxy acid $O-H$ stretch were detected in the present study. Either the experimental conditions employed were unfavorable for these reactions or the assumed mechanism for the formation of these novel hydroperoxy products is in error.

(iii) **Effect of O_2 on Product Distribution.** To further elucidate the mechanisms for the subsequent reactions of the primary radical $H_2C-O-\dot{C}H$, the yields of various products were measured as a function of O_2 partial pressure ranging from 0.01 to 100 Torr with O_2/N_2 total pressure maintained at 700 Torr. Illustrated in Figure 8 are the spectral data obtained in

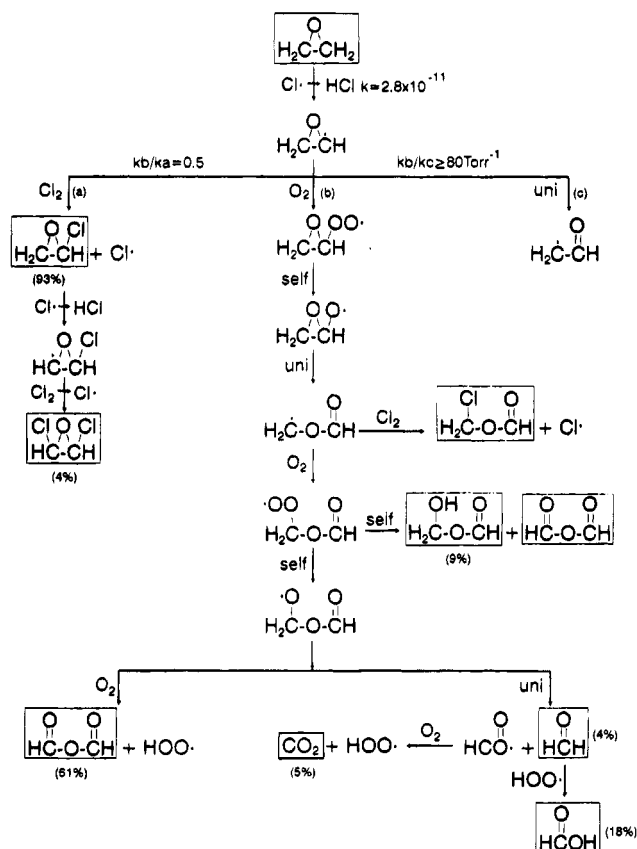


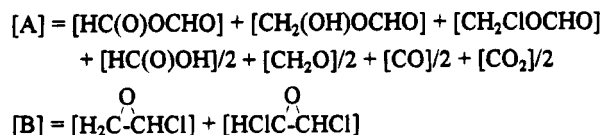
Figure 11. Mechanism for the Cl -atom-initiated reactions of ethylene oxide obtained in the presence of 0.02–2 Torr of Cl_2 in 700 Torr of N_2/O_2 mixtures. Numbers in parentheses are percentage yields of the products listed in Table 1.

the photolysis of a mixture containing $H_2C-O-CH_2$ (1 Torr), Cl_2 (0.5 Torr), and O_2 (10 Torr) diluted to 700 Torr with N_2 . Figure 8A,B shows the spectra recorded before and after 1 min irradiation, respectively; Figure 8C is the difference spectrum (8B–8A). The residual spectrum derived in this run is shown in Figure 6B, which exhibits peaks at 751, 945, 1126, 1267, 1771, and 2953 cm^{-1} . This spectrum is assigned to chloromethyl formate, $CH_2ClOCHO$, by comparison with the gas-phase spectrum reported by Dahlqvist.¹⁸ This compound can be taken as a unique product arising from Cl_2 reaction with the CH_2OCHO radical formed in reaction 6. Product yields determined for this run are listed in Table 1.

The yields of several products are plotted in Figure 9 as a function of O_2 partial pressure. The yields of $HC(O)OCHO$ and $H_2C-O-CHCl$ show positive and negative O_2 dependence, respectively. This observation is consistent with competition between the O_2 addition and Cl_2 reactions of the oxiranyl $H_2C-O-\dot{C}H$ radical (reactions 2 and 4). The O_2 dependence of the $HCHO$, $HC(O)OH$, and $CH_2ClOCHO$ yields exhibits a maximum, which can be qualitatively explained as follows. At a pressure of several torr of O_2 , the competition between reactions 2 and 4 determines the product distribution, so that an increase in O_2 pressure will increase the yields of O_2 -reaction products such as $HC(O)OCHO$, $CH_2ClOCHO$, $HCHO$, and $HC(O)OH$. At higher O_2 pressure, the competition between O_2 reaction and the unimolecular dissociation of the oxy radicals becomes more important to the product distribution, resulting in a net decrease in the observed yields of $HCHO$, $HC(O)OH$, and $CH_2(OH)OCHO$.

The rate constant ratio $k_4/k_2 = 0.5 \pm 0.1$ has been derived

from the slope of a plot $[A][Cl_2]$ vs $[B][O_2]$ (cf. Figure 10), where the terms $[A]$ and $[B]$ are defined as:



Here, $[A]$ represents the concentration of all the compounds produced via O_2 addition to the oxiranyl radical, and $[B]$, those arising from Cl_2 reaction with the oxiranyl radical. From this value for $k_4/k_2 = 0.5 \pm 0.1$ combined with $k_2/k_3 \geq 165 \text{ Torr}^{-1}$, the rate constant ratio for reactions 4 and 3 is estimated as $k_4/k_3 \geq 80 \text{ Torr}^{-1}$.

Conclusions

The experimental results demonstrate that, under atmospheric conditions, the oxiranyl radical $H_2C \overset{O}{\underset{||}{-}} O - CH$ is produced as the major primary radical from the $Cl + H_2C \overset{O}{\underset{||}{-}} O - CH_2$ reaction and that it undergoes predominantly O_2 addition rather than isomerization to vinoxy radical. A lower limit for the lifetime of the oxiranyl radical vs isomerization is estimated as $\geq 5 \times 10^{-5} \text{ s}$, and the rate constant ratio k_4/k_3 for O_2 addition vs isomerization, as $\geq 80 \text{ Torr}^{-1}$. Under the present experimental conditions, the resulting oxiranylperoxy radical $H_2C \overset{O}{\underset{||}{-}} O - C(OO)H$ was converted mainly to the oxy radical $H_2C \overset{O}{\underset{||}{-}} O - C(O)H$ via self-reaction. The epoxy ring of this oxy radical opens at the C—C bond rather than at the C—O bond, eventually leading to the formation of the ether-type (C—O—C) products $HC(O)OCHO$ and $CH_2(OH)OCHO$ and single carbon-containing oxidation products such as CO , CO_2 , $HCHO$, and $HC(O)OH$.

A summary of the mechanism derived in the present experiment is shown in Figure 11. This mechanism differs markedly from that of Bartels et al.¹ (Figure 1). However, it should be noted that Bartels' experiments were conducted in the absence of O_2 and that O_2 addition to the oxiranyl radical (reaction 4) was not operative. Also, in the present O_2 -free experiments, the concentration of Cl_2 (0.5 Torr) is much higher than that in Bartels' experiment (ca. $(1 \times 10^{-5}) - (1 \times 10^{-4})$ Torr). Therefore, unimolecular isomerization of the oxiranyl

radicals (reaction 3) was the dominant channel in Bartels' system, while bimolecular reaction with Cl_2 dominated in the present work.

Acknowledgment. We thank NSERC, AES, British Gas/Consumers Gas, and Ford Motor Co. for financial support for carrying out this work. H.N. is the holder of the British Gas/Consumers Gas/NSERC/AES Industrial Research Chair in Atmospheric Chemistry. We also thank Drs. H. O. Pritchard and D. Shen at York University for helpful discussions on thermochemical calculations.

References and Notes

- (1) Bartels, M.; Hoyer, K.; Lange, U. *Ber. Bunsen-Ges. Phys. Chem.* **1989**, *93*, 423.
- (2) Maker, P. D.; Niki, H.; Savage, C. M.; Breitenbach, L. P. *Am. Chem. Soc. Symp. Ser.* **1979**, *94*, 161.
- (3) Rannug, U.; Goethe, R.; Wachtmeister, C. A. *Chem. Biol. Interact.* **1976**, *12*, 251.
- (4) Derkosch, J.; Ernstbrunner, E.; Hoffmann, E. G.; Osterreicher, F.; Ziegler, E. *Monatsh. Chem.* **1967**, *98*, 956.
- (5) Niki, H.; Maker, P. D.; Savage, C. M.; Breitenbach, L. P. *J. Phys. Chem.* **1981**, *85*, 1024.
- (6) Su, F.; Calvert, J. G.; Shaw, J. H. *J. Phys. Chem.* **1980**, *84*, 239.
- (7) Lightfoot, P. D.; Cox, R. A.; Crowley, J. N.; Destriau, M.; Hayman, G. D.; Jenkin, M. E.; Moortgat, G. K.; Zabel, F. *J. Atmos. Environ.* **1992**, *26*, 1805.
- (8) Wallington, T. J.; Dagaut, P.; Kurylo, M. *J. Chem. Rev.* **1992**, *92*, 667.
- (9) Griesbaum, K.; Kibar, R.; Pfeffer, B. *Leibigs Ann. Chem.* **1975**, 214.
- (10) Chapman, O. L.; Adan, W.; Rodriguez, O.; Rucktaschel, R. *J. Am. Chem. Soc.* **1972**, *94*, 1365.
- (11) Dewar, M. J. S.; Zebisch, E. G.; Heuly, E. F. *J. Am. Chem. Soc.* **1985**, *107*, 3902.
- (12) Solly, R. K.; Golden, D. M.; Benson, S. W. *Int. J. Chem. Kinet.* **1970**, *2*, 11.
- (13) Batt, L.; Christie, K.; Milne, R. T.; Summers, A. *J. Int. Chem. Kinet.* **1974**, *6*, 877.
- (14) Kuhne, H.; Vaccani, S.; Ha, T. K.; Bauder, A.; Gunthard, H. H. *Chem. Phys. Lett.* **1976**, *38*, 449.
- (15) Kuhne, H.; Vaccani, S.; Bauder, A.; Gunthard, H. H. *Chem. Phys.* **1978**, *28*, 11.
- (16) Niki, H.; Maker, P. D.; Savage, C. M.; Breitenbach, L. P. *Chem. Phys. Lett.* **1980**, *75*, 533.
- (17) Atkinson, R.; Baulch, D. L.; Cox, R. A.; Hampson, R. F., Jr.; Kerr, J. A.; Troe, J. *J. Phys. Chem. Ref. Data* **1992**, *21*, 1125.
- (18) Dahlqvist, M. G. *Spectrochim. Acta* **1980**, *36A*, 37.
- (19) Baldwin, R. R.; Keen, A.; Walker, R. W. *J. Chem. Soc., Faraday Trans. 1* **1984**, *80*, 435.
- (20) Rossi, M.; Golden, D. M. *Int. J. Chem. Kinet.* **1979**, *11*, 715.

JP942218B